Available online at www.sciencedirect.com

SCIENCE DIRECT®

Journal of Nuclear Materials 320 (2003) 44–53

journal of nuclear materials

www.elsevier.com/locate/jnucmat

The chemistry and physics of modelling nitride fuels for transmutation

Roger Thetford [a,*], Mike Mignanelli [b,1]

[a] Serco Assurance, 150 Harwell Business Centre, Didcot OX11 0QJ, UK
[b] AEA Technology, 168 Harwell Business Centre, Didcot OX11 0QJ, UK

Abstract

Against the background of increased interest in nitride fuel for transmutation of minor actinides, this paper presents the current status of UK modelling of nitride fuel pins. A new equilibrium chemistry model for nitride fuel, suitable for inclusion in fuel pin modelling codes, is described. High-temperature experiments on (U,Zr)N in a sealed capsule indicate that actinide nitrides in a nitrogen atmosphere are stable up to their melting point. The paper also recommends a set of physical and chemical properties for advanced nitride fuels, highlighting the areas where data are presently missing.

PACS: 28.41.Ak; 62.20.–x; 64.90.+b; 65.50.+m

1. Introduction

There is a strong European background in fast reactors fuelled with $(U,Pu)O_2$. However, the emphasis is moving away from power generation and towards the burning of plutonium and minor actinides. Using nitrides as a fuel in a fast transmutation reactor offers potentially enhanced performance compared to the more conventional oxide fuel due to the higher thermal conductivity, good sodium compatibility and, in the case of fuel reprocessing, high solubility in nitric acid. The different fuel options that are being considered include (U,Pu)N, PuN, (Pu,Zr)N, (Pu,Am)N and (Pu,Ac,Zr)N, where Ac represents the minor actinides such as Np, Am and Cm; Zr is added as a diluent. These fuels all form single-phase solid solutions for normal irradiation conditions. Heterogeneous nitride fuels (e.g. CERCER fuel PuN with Si_3N_4) are of secondary interest.

The thermophysical behaviour and stability of homogeneous fuels during irradiation requires attention, particularly for reactor scenarios that result in abnormal temperature transients [1]. The main issues of concern are solid fission product swelling, fission gas retention in the fuel and stability of the fuel at high temperatures. Because of the present lack of irradiation data on minor actinide fuels, modelling will inevitably be required. But such modelling should be soundly-based, including the chemical effects of introducing the minor actinides and of moving from oxide fuels to nitrides. For example, the chemical state of the fuel affects the solid fission product swelling, which in turn affects the local stress calculation – particularly if the fuel–clad gap is closed. Volatile species will tend to migrate outwards towards the gap, where they can accumulate (and/or move axially), affecting the gap conductance.

Modelling codes also need the physical properties of these fuels. Some of the physical properties are poorly-known; others are missing completely and must be extrapolated from known information.

This paper describes a new equilibrium chemistry model for nitride fuel, and the theory-based extension of some high-temperature stability experiments for (U,Zr)N to other actinides. It also recommends a set of

---

* Corresponding author. Tel.: +44-1635 280439; fax: +44-1635 280302.

E-mail address: roger.thetford@sercoassurance.com (R. Thetford).

[1] Tel.: +44-1235 432421; fax: +44-1235 433530.

0022-3115/03/$ - see front matter © 2003 Elsevier Science B.V. All rights reserved.
doi:10.1016/S0022-3115(03)00170-3

physical properties for actinide nitrides in solid solution with a ZrN diluent, and highlights the areas where further experiments are needed to increase confidence in the underlying properties.

The chemical model and the recommended physical properties described here are implemented in the NITRAF code [2], which is evolving as part of the EC Fifth Framework Project CONFIRM [3].

2. Chemical state of nitride fuels

Matzke has reviewed the available information on the chemical state of the fission products in carbide and nitride fuels and their influence on fuel properties [4]. The review also includes data on the redistribution of fission products during irradiation, solid fission product swelling and clad corrosion. Some of the main findings on nitride fuel are summarised in the following sections.

2.1. U–Pu nitride fuel

The U–Pu–N system can be considered in three separate regions; the two-phase region metal and mononitride; the single-phase solid solution region; and the sesquinitrides. The mononitrides UN and PuN are the main phases of interest and exist over a narrow composition range and therefore it is reasonable to assume that this is the case for the solid solution. The mononitride shows complete miscibility over the entire composition range. No sesquinitrides of plutonium have been reported.

2.2. Soluble fission products

Benedict has reviewed the experimental data on fission product solubilities in nitride fuel [5,6]; this also included predictions for elements for which no data are available. A simple rule was established that compares the crystal structure and lattice parameter of the solute nitride, MeN_y, with that of the fuel nitride, MN_y ($y = N/(M$ or $Me)$ and $M = U$ or Pu). Only solute nitrides with the same crystal structure as the fuel are considered soluble and the extent of solubility derived from an assessment of the difference between the lattice parameters (a, measured at room temperature) of the solute and solvent nitrides (RLPD – relative lattice parameter difference),

$$\mathrm{RLPD} = \frac{a(\mathrm{MeN_y}) - a(\mathrm{MN_y})}{a(\mathrm{MN_y})}.$$

Complete solubility is observed for a RLPD between −7.5% and +8.5% and solubility is negligible for a RLPD more negative than −16%.

Based on the available experimental measurements performed on samples quenched from 1600 °C, the following nitrides show complete miscibility in UN and hence solid solution formation; YN, LaN, CeN, PrN, NdN and ZrN. The remaining elements of the rare earth series are predicted to be miscible. The maximum solubility of NbN in UN has been measured as 50 mol% and hence fission product Nb should be completely dissolved in the fuel lattice. The lattice parameter of UN is increased by the rare earths (with the exception of YN which has a lattice parameter very close to that of UN) and lowered by ZrN and NbN. Some slight deviations from the Vegard Law line are observed; CeN shows negative deviation which is attributed to valence changes of Ce. In general the solubility behaviour of these solutes in PuN is assumed to be similar.

2.3. Insoluble fission products

Sintered compacts of PuN–Mo and UN–Mo were heat treated at 1700 °C for 6 h under nitrogen and quenched [5,6]. A small lattice parameter decrease was observed for all Mo concentrations in PuN. No significant changes were determined for the UN samples (solubility of Mo in nitride fuel is less than ~0.1 wt%).

The noble metal group (Ru, Rh, Pd, Pt) are, next to the rare earths, the second most abundant of the fission products. However, no nitride phases have been reported and hence these elements could precipitate out during irradiation as intermetallic phases, such as $(U,Pu)Pd_3$ or $(U,Pu)(Pd,Rh,Ru)_3$ possibly including some Mo and Tc.

No solubility data are available for the alkaline earths, Sr and Ba, in nitride fuel. These fission products are assumed to precipitate as the nitride phases Sr_3N_2 and Ba_3N_2 respectively in regions of the fuel where there is sufficient diffusion of the metal to the grain boundaries.

2.4. Volatile fission products

The volatile fission products include the rare gases (Kr, Xe), the halogens (Br, I), the alkali metals (Rb, Cs) and the chalcogenides (Te, Se). The halogen and alkali metal groups do not form nitrides but tend to form compounds with the other volatile elements, such as CsI. Only the chalcogenides form nitrides (SeN_x and Te_3N_4) but these probably decompose even at low temperatures. Therefore in irradiated nitride fuel Se and Te are expected to be present in either elemental form or in compounds with the other volatile elements (e.g. Cs_2Te).

In oxide fuels, the mobility of molybdenum has been attributed to the formation of volatile caesium molybdate and gaseous diffusion along cracks and interconnected porosity. But in nitride fuels, oxidation of the fuel is excluded and therefore compounds such as caesium molybdates, caesium uranates and caesium chromates will not form. Therefore the mobility of the volatile fission products will depend on their partial pressures over the binary phases (Cs_2Te, CsI); consequently the mobility of Mo will tend to be less than that for oxide fuels.

2.5. Effect of impurities

The main impurities likely to be introduced during the nitride fabrication process are carbon and oxygen. The influence of such impurities on the fuel properties of UN and $(U_{0.8}Pu_{0.2})N$ has been investigated by Arai et al. [7]. Based on lattice parameter results, carbon up to 0.2 wt% is assumed to dissolve in the mononitride lattice; no carbide phases were identified. However, it was confirmed that samples containing up to 1 wt% oxygen (equivalent to $MN_{0.84}\ O_{0.16}$) in the fuel form oxide precipitates and the amount of dissolved oxygen does not change with added oxygen content. The solubility limit of oxygen in the mononitride is limited (7 at.% UO in UN and 14 at.% PuO in PuN). The average grain size of the matrix phase decreases with increase in oxygen content and the thermal conductivity of the pellets containing 1 wt% oxygen is lower by $\sim$9.5% and 12.5% at 1000 and 1500 K respectively compared to nitride pellets containing up to 2000 ppm oxygen. However, such high levels of oxygen contamination would not be acceptable for the nitride fabrication process.

2.6. Cladding components

A number of mechanisms have been proposed for the chemical corrosion of the clad in oxide fuel pins. The extent of fuel–clad chemical interaction (FCCI) was dependent on the oxygen potential in the fuel–clad gap (hence oxygen-to-metal ratio), the temperature, clad composition and extent of migration of the volatile fission products (e.g. Cs and Te). The transfer of nitrogen from nitride fuel to the clad appears to be less of a problem than clad oxidation is for oxide-fuelled pins. Irradiation experience, which includes sodium-bonded pins and out-of-pile tests, confirm the good compatibility of mononitride fuel with stainless steel. There have been some observations of a thin nitrided inner zone of the clad [4] in inert gas bonded pins but this did not result in a deterioration of the mechanical properties of the clad.

Hypostoichiometric fuel, MN_{1-x}, contains free metal and hence should be avoided since a eutectic melting reaction can occur with the clad [8]. Hyperstoichiometric U,Pu nitrides containing sesquinitrides are predicted to nitride the clad components in inert-gas-bonded pins, the extent depending on the nitrogen partial pressure and the temperature. Chromium nitride precipitates (CrN, Cr_2N) have been observed in the clad but with no apparent detrimental effects. There would be an increased potential for nitriding in nitrogen-bonded pins. The N/M ratio is expected to increase with burn-up and hence the amount of sesquinitride (essentially U_2N_3 as the plutonium sesquinitride has not been characterised) should also increase with burn-up. However, no excessive clad corrosion has been observed with nitrides irradiated to high burn-ups.

2.7. Irradiation effects

A comparison of the chemical constitution of irradiated U,Pu nitride fuel with oxide and carbide fuels [9] shows that the nitride has significantly fewer fission product phases even at compositions simulating 10% burn-up. This reflects the higher solubility of the rare earths in the (U,Pu)N fuel and the lack of formation of ternary phases (cf. zirconates, uranates in oxide fuel). Volume changes due to the dissolution of fission products were also found to be small; lattice parameter measurements have shown that the increase in a_0 due to the rare earths is compensated by the decrease due to Zr. Thermodynamic calculations of the chemical state of nitride fuel at 1000 K indicate an increase in volume of 0.53% per one percent increase in burn-up. Similar calculations also predict an increase in the overall N/M ratio to 1.047 after 10% burn-up [9]. In the case of uranium-containing fuels this excess would be accommodated by the formation of the sesquinitride phase. However, for uranium-free fuel the excess nitrogen would be released to the pin plenum.

The radial redistribution of fuel and fission products along a severe temperature gradient is well-known for oxide fuels. In nitride fuels the temperature gradients are significantly smaller and therefore less U and Pu and also pore mobility is expected. In general this is also the case for the fission products. However, due to the reducing conditions of nitride fuels the transport of some fission products, in particular Cs and the alkaline earths, is enhanced. Stable ternary phases that are found in oxide fuels (e.g. caesium uranates, caesium molybdates and barium zirconates) do not form and hence the vapour pressures of elemental Cs, Te, Ba and Sr are higher in nitrides. Radial transport occurs by an evaporation–condensation mechanism and is faster in high-power conditions.

3. A chemical model for nitride fuels

The chemical behaviour of the fuel and fission products in oxide fuel was modelled in TRAFIC by the Alchemist routines [10]. The routines are based on the chemical equilibrium program SOLGASMIX [11] and adapted for modelling $(U,Pu)O_{2\pm x}$ fuel and the fission product elements. It is not possible to model all of the components of the fuel pin and so representative elements of the fission products are selected. The fundamental parameters required for the calculations are thermodynamic data for the phases formed in the fuel during the irradiation. A similar approach was adopted to model the chemistry in NITRAF and this can be compared with the thermodynamic assessment of irradiated nitride fuel performed by Schram and Konings [12].

The inventories of the representative elements, which include the minor actinides (i.e. N, Xe, Cs, I, Te, Sr, Ba, U, Np, Pu, Am, Cm, La, Ce, Zr, Mo and Ru), are calculated using equations derived from the FISPIN code [13]. In the case of the clad, the amounts of Fe, Cr and Ni are based on a nominal composition. The thermodynamic parameters for most of the species in the system, included in the format $G - H_{SER}$ (Gibbs energy relative to a reference state), are available but data for NpN, AmN and CmN were estimated. In the first release of the code the components of the mononitride phase, $MN_{\langle solid\rangle}$, are assumed to form an ideal solid solution. Although ZrN is included in the database it is assumed to represent the dissolution of fission product zirconium as a dilute ideal solution in the actinide matrix. A more detailed assessment of the solution behaviour is required in order to represent ZrN as a diluent material initially present in the fuel. Other solution phases included in the model are $MN_{\langle liquid\rangle}$, $M_{\langle liquid\rangle}$ (U, Np, Pu, Am, Cm, La, Ce, Zr, Sr, Ba, Cs and Te), $M_{\langle alloy\rangle}$ (Mo and Ru solution) and $M_{\langle clad\rangle}$ (Fe, Cr and Ni solution).

The total yields of the representative elements are determined first. For elements that remain in solution in the nitride fuel lattice, the full inventories are included in the equilibrium calculation. For less-soluble groups, the amounts available for reaction are less than the full inventories, recognising that some material (in amounts controlled by diffusion from the fuel lattice) will be precipitated at the grain boundaries. In the cooler outer regions of the fuel the diffusion of these fission products is slow and hence would not contribute significantly to the formation of condensed phases. These processes are treated in NITRAF using models for rare gas diffusion and experimentally-determined effective diffusion coefficients. The latter were obtained for the release of Xe, Cs, I, Te and Mo in trace-irradiated polycrystalline urania [14,15] and are assumed to be appropriate for nitride fuel; this assumption will require further assessment at a later stage.

The temperature, pressure and pore structure (which affects the transport of volatile species and hence the chemical equilibrium) vary axially and radially through the fuel. As irradiation proceeds, NITRAF determines the chemical constitution of the fuel and clad for each radial fuel and clad ring at each axial level, at a series of burn-up steps. The chemical state of a fuel ring is based on the determination of the equilibria of the fuel and fission product system at the calculated temperature and pressure conditions. NITRAF uses a calculation scheme similar to that used in the oxide version of the code. However, in place of the 'fixed oxygen potential' calculation used for oxide fuels, where significant oxidation of the cladding could occur, for nitrides it is assumed that the total nitrogen content in the fuel and clad in an axial section is constant.

The equilibrium composition of the innermost (hottest) nitride fuel ring is determined first, using the elements soluble in the fuel lattice and a proportion of the less soluble groups determined from diffusion behaviour. The composition of the next ring is calculated in the same way, but adding to the starting inventory an amount of the gas phase species from the previous ring based on a gaseous diffusion model. These calculations are continued until the outer fuel ring is reached. The total nitrogen inventory required for the given conditions in the fuel rings is summed and any remaining nitrogen is then included in the clad ring calculation. In the initial version of the nitride chemistry model, an axial migration model that partitions the species in the gas phase along the axial fuel–clad gap is not included.

The extent of fuel swelling due to fission product effects is estimated from the equilibrium amounts and densities of the fuel solid solution and condensed phases formed at the grain boundaries. The influence of fuel–clad chemical interaction on the reduction of clad thickness is also estimated from the amounts of the condensed nitride species involving clad components (e.g. Fe_2N, Fe_4N, CrN, Cr_2N and Ni_3N) that are formed at the different axial positions along the pin.

4. Implementing the chemical model in NITRAF

This section presents the results of test calculations of the chemical composition of nitride fuel as a function of temperature using the preliminary chemistry models. The initial fuel composition was one mole of the U,Pu mononitride comprising small amounts of the minor actinides, $(U_{0.45}Pu_{0.45}Np_{0.04}Am_{0.04}Cm_{0.02})N$, and the chemical state was calculated after 20 at.% burn-up and for a range of temperatures. Clad components Fe, Cr and Ni were also included as input species in the ratio appropriate to 316 stainless steel and the fill gas of the pin was assumed to be inert.

The results of the equilibrium chemistry calculations for temperatures between 800 and 2100 K are shown in Fig. 1. The main condensed phase formed is the fuel solid solution MN that comprises U, Pu, and the minor actinides, and the dissolved fission products Ce, La and Zr. The concentration of uranium in the MN phase changes due to the formation of UN1.59 (i.e. the

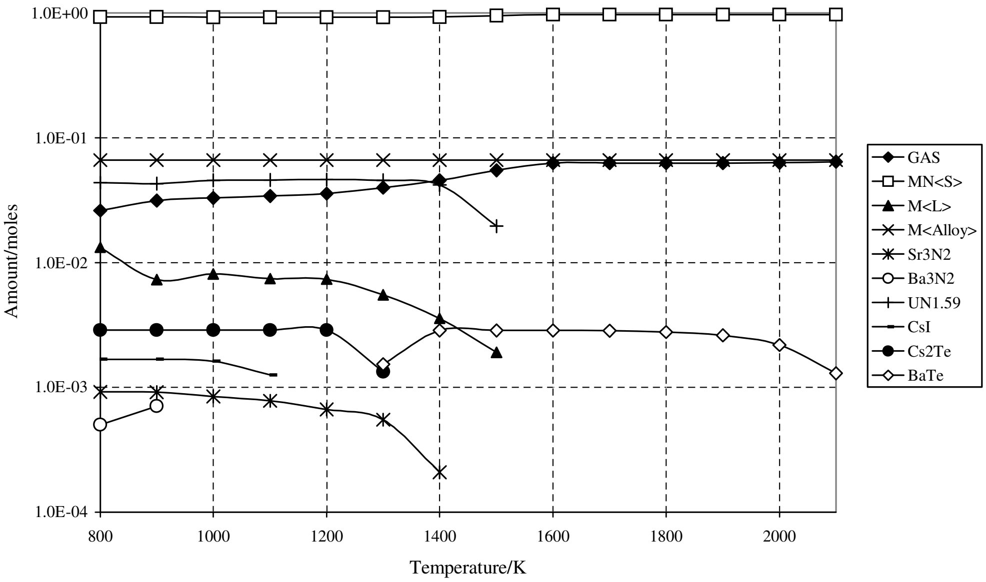

Fig. 1. Variation of mononitride fuel composition with temperature.

uranium sesquinitride) at the lower temperatures. The sesquinitride is stable up to ~1673 K and above this temperature only the mononitride is stable. The formation of other nitride compounds of the fission products is limited for the reducing conditions of the nitride fuel; both Sr_3N_2 and Ba_3N_2 are stable only at low temperature (<1473 and <1073 K respectively). Strontium nitride dissociates to form the metal phase which is stable up to ~1800 K and at higher temperatures gaseous species of Sr are formed (e.g. $Sr_{\langle g \rangle}$ and $SrI_{\langle g \rangle}$). Similar behaviour occurs in the case of the barium nitride phase although the calculations predict the formation of the BaTe phase at high temperature. Molybdenum and ruthenium remain as the metal phase under these conditions. The more volatile fission products Cs, I and Te occur as stable condensed phase species, Cs_2Te and CsI, up to ~1400 K and form gaseous species at higher temperatures. The gas phase is dominated by N_2, Xe, Cs, Te, I, Sr and Ba species. These results are consistent with the observations of the chemical state of irradiated and simulant nitride fuel [4] and the calculations performed by Schram and Konings [12]. No clad nitrides are predicted to form.

Similar calculations performed on fuel without UN initially present have also been performed (U-free fuel). In this case the excess nitrogen formed during irradiation is not consumed by the formation of the sesquinitride at low temperatures and clad nitrides are predicted to form (e.g. CrN). At high temperatures (>1200 K) these phases are unstable and the excess nitrogen is released to the pin plenum.

5. Physical properties

A model of a fuel pin under irradiation must represent a number of physical processes as well as the chemical processes discussed above. The most important are the removal of heat by thermal conduction and the mechanical behaviour of the fuel and cladding. But in high burn-up fuel for transmutation reactors, restructuring, grain growth, solid swelling and gas behaviour (of both fission gas and decay-generated helium) have increasingly significant effects.

The thermomechanics of the fuel are determined principally by its thermal expansion, specific heat, thermal conductivity, creep and elastic constants. Fracture stresses also play a part. Physical restructuring of the fuel is caused by bubble motion, which depends on surface energies and vapour pressures, and on solid-state and gas–atom diffusion within the matrix. Redistribution of the fuel components depends on diffusion constants and heats of transport.

Ideally, all of these properties should be available for a candidate fuel material, as a function of composition (including minor actinides, diluents and inert matrices, and any deviation from the ideal stoichiometry), temperature and burn-up. In practice, linear combinations of properties of pure materials are often used. The remainder of this section makes a new recommendation for the melting points of actinide and zirconium nitrides, then summarises the current position on the other physical properties of nitride fuels.

5.1. Melting points of nitride fuels

A full safety case for fuelling reactors with nitride fuel requires calculations of overpower transients and behaviour up to and beyond fuel melting. The existing literature [4,16–40] does not include any data on the melting temperatures of mixed-actinide nitrides containing a zirconium diluent.

Experimental determinations of the solidus and liquidus temperatures of $U_{0.2}Zr_{0.8}N$ have been conducted recently [41], involving the thermal treatment of samples of the mixed nitride in welded tungsten capsules up to ~2800 °C using RF heating. There was no indication of any reactions or damage to the capsules after the test and the solidus and liquidus temperatures were determined at 2612 and 2765 °C respectively. A tentative UN–ZrN phase diagram was proposed based on the thermodynamic data for the system, non-ideal solution behaviour and the experimental results for $U_{0.2}Zr_{0.8}N$; the eutectic point is calculated from the optimisation of these data. The behaviour of (Pu,Zr)N solid solutions at high temperatures was also assessed from these experimental data. Using the same interaction terms for the liquid and solid solution phases derived in the model for the UN–ZrN system and the thermodynamic data for PuN, solidus and liquidus temperatures were estimated for (Pu,Zr)N compositions. The results indicated that up to ~2500 °C liquid phase is not formed for fuel containing 20–40 mol% PuN but this would need to be confirmed experimentally.

Fig. 2 shows the phase diagram for (U,Zr)N based on the thermodynamic calculations. Let z be the fraction of Zr. The eutectic point is approximately 2885 K, for $z = 0.5471$. Given the lack of evidence, a burn-up of b% fissions per initial metal atom (fima) is assumed to have the same effect as in oxide fuel [42], i.e. to reduce the melting temperatures by $3.4b$ K. The left-hand and right-hand parts of each curve have been fitted separately with quartic polynomials in $x = (z - 0.5471)$, giving the recommendations

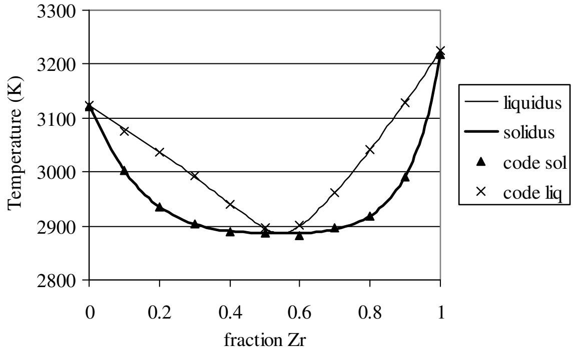

Fig. 2. Solidus and liquidus temperatures of (U,Zr)N: recommendation in this paper (points) compared to phase diagram from thermodynamic calculations (lines).

$$T_{\mathrm{sol,U}} = \begin{cases} 1193.9x^4 - 975.69x^3 - 147.51x^2 \\ \quad -28.418x + 2885.8 - 3.4b \quad (x < 0), \\ 27618x^4 - 15672x^3 + 3481.7x^2 \\ \quad -193.96x + 2885.8 - 3.4b \quad (x \geqslant 0), \end{cases} \tag{1}$$

$$T_{\mathrm{liq,U}} = \begin{cases} 6387.5x^4 + 7371.0x^3 + 2698.2x^2 \\ \quad -117.93x + 2885.8 - 3.4b \quad (x < 0), \\ 6607.9x^4 - 7494.3x^3 + 3418.9x^2 \\ \quad +125.97x + 2885.8 - 3.4b \quad (x \geqslant 0). \end{cases} \tag{2}$$

Calculated points using these recommendations are also shown in Fig. 2, labelled ‘code sol’ and ‘code liq’.

The calculated phase diagram for the PuN–ZrN system is similar, with the eutectic composition determined at $z = 0.4922$. Fitting the left-hand and right-hand parts of each curve separately with quartic polynomials in $y = (z - 0.4922)$ gives

$$T_{\mathrm{sol,Pu}} = \begin{cases} 1316.6y^4 - 997.38y^3 - 64.914y^2 \\ \quad -15.163y + 2804.1 - 3.4b \quad (y < 0), \\ 29782y^4 - 20579y^3 + 5004.7y^2 \\ \quad -331.42y + 2804.1 - 3.4b \quad (y \geqslant 0), \end{cases} \tag{3}$$

$$T_{\mathrm{liq,Pu}} = \begin{cases} 7916.1y^4 + 7967.4y^3 + 2565.8y^2 \\ \quad -104.74y + 2804.1 - 3.4b \quad (y < 0), \\ 6181.4y^4 - 7535.2y^3 + 3525.5y^2 \\ \quad +175.16y + 2804.1 - 3.4b \quad (y \geqslant 0). \end{cases} \tag{4}$$

There are sparse data only for the melting points of the pure minor actinide nitrides. Following the chemical similarities between other actinide compounds, the melting point of (Np,Zr)N can be assumed to be the same as (U,Zr)N, and (Am,Zr)N and (Cm,Zr)N the same as (Pu,Zr)N.

5.2. Nitride fuels: existing recommendations

Some physical properties have been measured for UN and PuN, but there are scarcely any data for the minor actinide nitrides. The unpublished reviews [43–45] make recommendations for (U,Pu,Zr)N based on the published literature [4,16–40]. The recommendations are listed here for the first time in Table 1. Properties of (U,Pu,Zr)N are calculated from linear combinations of the actinide and zirconium data, with the exception of the creep, elastic moduli, self-diffusion and thermal conductivity where ZrN data are missing or unreliable and the (U,Pu)N data are used instead. Apart from density, the only properties found for minor actinide nitrides were very close to the data for (U,Pu)N, so the (U,Pu)N data were extended to

Table 1
Recommendations for physical properties

Quantity	Recommended expression	References and notes
Lattice parameter at 298 K (nm)	0.4889 (UN), 0.49049 (PuN), 0.4998 (AmN), 0.48969 (NpN), 0.5034 (CmN)	[4,20,46–49]; note 1
Theoretical density at 298 K (kg m^{-3})	14 330 (U^{14}N), 14 250 (Pu^{14}N), 13 570 (Am^{14}N), 13 440 (Cm^{14}N), 14 450 (Np^{14}N), 7030 (Zr^{14}N) 14 380 (U^{15}N), 14 300 (Pu^{15}N), 13 630 (Am^{15}N), 13 490 (Cm^{15}N), 14 510 (Np^{15}N), 7370 (Zr^{15}N)	[4,20,46–49]; note 1
Length $L(T)$ (thermal expansion)	$L(298)[0.9980 + 6.43 \times 10^{-6}T + 1.89 \times 10^{-9}T^2]$ for AcN $L(298)[0.9983 + 5.27 \times 10^{-6}T + 1.15 \times 10^{-9}T^2]$ for ZrN	[4,16,20,21,32–34,38]; notes 1,2,3
UN enthalpy (J mol^{-1})	$H(T) - H(298) = 3.007 \times 10^{-9}T^4 - 1.387 \times 10^{-5}T^3 + 2.939 \times 10^{-2}T^2 + 3.038 \times 10^{1}T - 9.438 \times 10^{3} - \frac{5.637\times10^5}{T}$	[19,22,23]; note 4
(Pu,Am,Cm,Np)N enthalpy (J mol^{-1})	$H - H(298) = 45.002T + 7.710 \times 10^{-3}T^2 - 1.410 \times 10^4$	[4,23,50]; note 5
ZrN enthalpy (J mol^{-1})	$H - H(298) = 44.007T + 3.999 \times 10^{-3}T^2 - 3.7877 \times 10^5$	[39,45]
UN heat capacity (J mol^{-1} K^{-1})	$C_p = 1.203 \times 10^{-8}T^3 - 4.161 \times 10^{-5}T^2 + 5.877 \times 10^{-2}T + 3.038 \times 10^1 + 5.637 \times 10^5/T^2$	[19,22,23]; note 4
(Pu,Am,Cm,Np)N heat capacity (J mol^{-1} K^{-1})	$C_p = 45.002 + 1.542 \times 10^{-2}T$	[4,23,50]; note 5
ZrN heat capacity (J mol^{-1} K^{-1})	$C_p = 44.007 + 7.998 \times 10^{-3}T$	[35,45]
Thermal conductivity for fully-dense (U,Pu,Zr)N (W m^{-1} K^{-1})	$k_0 = AT^2 + BT + C$ where $A = 4.558 \times 10^{-5}y^3 - 7.734 \times 10^{-5}y^2 + 4.180 \times 10^{-5}y - 1.159 \times 10^{-5}$, $B = -1.044 \times 10^{-1}y^3 + 1.726 \times 10^{-1}y^2 - 9.464 \times 10^{-2}y + 3.307 \times 10^{-2}$, $C = 5.852 \times 10^1y^3 - 8.291 \times 10^1y^2 + 3.051 \times 10^1y + 1.326$	[4,20,24,32–34, 38,45,50,51]; note 6
Effect of porosity on thermal conductivity	$k = k_0 f(p)$ where $f(p) = \frac{1-p}{1+2p}$	[4,20,24,38]
(U,Pu,Zr)N Young's modulus (GPa)	$E = 280(1.0274 - 0.92 \times 10^{-4}T)(1 - 2.7p)$	[4,45]; notes 7,8
(U,Pu,Zr)N Shear modulus (GPa)	$G = 110(1.0274 - 0.92 \times 10^{-4}T)(1 - 2.62p)$	[4,45]; notes 7,9
(U,Pu,Zr)N creep (s^{-1})	$\dot{\varepsilon} = \exp(25p)[6.46 \times 10^{-6}\sigma^6 \exp(-37750/T) + 5.33 \times 10^{-32}\sigma\dot{F}]$	[4,19,20,25,26,45]; notes 7,10
(U,Pu,Zr)N self-diffusion D (m^2 s^{-1})	$D = 1.545 \times 10^{-10}\exp(-34094/T) + 1.8 \times 10^{-40}\dot{F}$	[4,45]; notes 7, 11
Inert gas atom diffusion in (U,Pu)N (m^2 s^{-1})	$D_{\mathrm{Xe,nitride}} = 1.143 \times 10^{-7}\exp(-35\,225/T)$	[39]; note 7
Grain growth dd/dt (m s^{-1})	$\frac{\mathrm{d}d}{\mathrm{d}t} = \frac{1.49\times10^{-18}}{d^2}\exp(-13\,403/T)$	[4]; note 2
Maximum clad internal corrosion	1 µm/% burn-up (fima)	[44]; note 12
Diffusion of atomic nitrogen in fuel matrix (m^2 s^{-1})	$D_{\mathrm{nitrogen}} = 3 \times 10^{-8}\exp(-31\,680/T)$	[4]; note 13
Note 1	Unless otherwise stated, properties of the mixed solid solution (Ac,Zr)N should be interpolated using Vegard's law from the properties of UN, PuN and ZrN. Where there are no data, treat Np as U, Am and Cm as Pu.	
Note 2	Apply (U,Pu)N expression to minor actinides.	
Note 3	(U,Pu)N data sparse and scattered, no evidence of variation with Pu content. Valid 293 to 2836 K (ZrN).	
Note 4	Valid up to 2650 K. Uncertainties in heat capacity of ±2 J mol^{-1} K^{-1} up to 1500 K, rising to ±6 J mol^{-1} K^{-1} at 2650 K.	
Note 5	Based on measurements up to 1562 K, but given lack of other data, use this recommendation at higher temperatures too. Uncertainties in C_p±5 J mol^{-1} K^{-1} up to 1562 K, rising to ±10 J mol^{-1}K^{-1} at 2650 K.	

Note 6	No (U,Pu)N data above 1600 K; extrapolate to 2650 K. Uncertainty ±0.5 $\mathrm{W\,m^{-1}\,K^{-1}}$ up to 1600 K, rising to ±1.5 $\mathrm{W\,m^{-1}\,K^{-1}}$ at 2650 K. The expressions given were developed for (U,Pu,Zr)N with y as the fraction Pu/(U + Pu + Zr). Ref. [50] shows conductivities decreasing with atomic number. Apply the standard expressions to mixed actinides too: speculate that the trend continues and set $y = \left(\frac{1}{2}\mathrm{Np} + \mathrm{Pu} + \frac{3}{2}\mathrm{Am} + 2\mathrm{Cm}\right)/(\mathrm{U} + \mathrm{Np} + \mathrm{Pu} + \mathrm{Am} + \mathrm{Cm} + \mathrm{Zr})$, subject to $y \leqslant 1.5$ to prevent extreme extrapolation.
Note 7	Apply (U,Pu)N data to ZrN.
Note 8	Uncertainty ± 10 GPa at 298 K, ±20 GPa at 1500 K.
Note 9	Uncertainty ± 5GPa at 298 K, ±10 GPa at 1500 K.
Note 10	Data for UN only; apply to AcN. Measured over the range 1773–2073 K; uncertainty is a factor of 4 or 5.
Note 11	Uncertainty is a factor of 10 on thermal term, 28% (i.e. coefficient is $(1.8 \pm 0.5) \times 1 \times 10^{40}$) on irradiation term.
Note 12	For AIM1 and 15/15Ti cladding, at the position of maximum corrosion.
Note 13	Not used in NITRAF because this is three orders of magnitude slower than the solid-state diffusion of oxygen; rely on chemical-kinetic vapour diffusion model instead.

In the expressions above, T is the temperature (K), $L(T)$ is length at temperature T, p is the fractional porosity in the fuel, σ the applied (von Mises) stress (MPa), $\dot{F}$ the fission rate (fissions $\mathrm{m^{-3}\,s^{-1}}$), d the grain diameter (m).

apply to the general actinide nitride. For density, theoretical densities were calculated from the measured lattice parameters [46–49] and the molecular weights.

Some of the quantities necessary for a fuel performance model are missing from Table 1. Oxide data (for UO_2 or $(U,Pu)O_2$) are used for fracture stress, heats of transport, densification, grain boundary diffusion rates, grain boundary and surface energies, and are not presented here. Also, the oxide fuel model is used for the conductance of the gap between nitride fuel and the cladding.

Recent Japanese work [50,51] indicates that the thermal conductivity of NpN lies between that of UN and PuN, and the heat capacity is almost the same as that of UN and PuN.

The most significant omission in the literature reviewed here is the thermal properties of AmN: thermal conductivity, linear expansion and heat capacity. The similar gaps for curium are less important because of its likely lower concentration in a transmutation fuel. Information on the evolution of physical properties with burn-up is also lacking.

6. Conclusions

An equilibrium chemistry model has been written for the nitride fuel pin modelling code NITRAF. A calculation using the new model for fuel containing uranium shows that for the test conditions considered, the surplus of nitrogen produced during irradiation is absorbed into the fuel as the uranium sesquinitride and no clad nitrides are predicted to form. For uranium-free fuels, the surplus nitrogen reacts with the clad at low temperatures to form clad nitrides; above 1200 K these phases dissociate, releasing the excess nitrogen to the pin plenum.

Recommendations have been made for many of the physical properties needed to model nitride fuels for transmutation. However, experimental data are scarce. The most significant omissions are the thermal conductivity, linear expansion and heat capacity of americium nitride. Some data are also lacking for diluent materials, which are much easier to experiment with: for example, measurements of the creep, elastic moduli and more complete measurements of the thermal conductivity of ZrN would be very useful.

Data from post-irradiation examination of advanced nitride fuels may permit the construction of empirical fuel performance models. However, extending such models from the burn-up or temperature ranges for which they were fitted to the more demanding conditions of a full-scale actinide burner is risky. Soundly-based physical models like those developed for $(U,Pu)O_2$ fuels are likely to give better results – provided that the physical properties are known.

Acknowledgements

This work was jointly funded by British Nuclear Fuels plc and the Fifth Framework Programme (Nuclear Fission) of the European Commission, contract FIKW-CT2000-00096.

References

[1] J. Wallenius, K. Tucek, W. Gudowski, Sixth International Information Exchange Meeting on Actinide and Fission Product P&T, Madrid 2000.

[2] M.A. Mignanelli, R. Thetford, D.A. Williams, Fuel performance modelling of nitride fuels, Proceedings of the International Conference, Global'99, Chicago, September 1999.

[3] http://clio.neutron.kth.se/CONFIRM/.

[4] Hj. Matzke, Science of Advanced LMFBR Fuels, North Holland, Amsterdam, 1986.

[5] U. Benedict, The solubility of solid fission products in carbides and nitrides of uranium and plutonium, Part I: Literature review on experimental results, Euratom Report EUR-5766 e, 1977; Part II: Solubility rules based on lattice parameter differences, Euratom Report EUR-5766 EN, 1977.

[6] U. Benedict, in: Thermodynamics of Nuclear Materials 1979, vol. 1, IAEA, Vienna, 1980, p. 453.

[7] Y. Arai, M. Morihira, T. Ohmichi, J. Nucl. Mater. 202 (1993) 70.

[8] J. Henshaw, M.A. Mignanelli, AEA Technology Report AEAT-0075, March 1996.

[9] M.H. Bradbury, Hj. Matzke, J. Nucl. Mater. 91 (1980) 13.

[10] M.A. Mignanelli, R. Thetford, J. Nucl. Mater. 204 (1993) 173.

[11] G. Eriksson, Chemica Scripta 8 (1975) 100.

[12] R.P.C. Schram, R.J.M. Konings, Proceedings of Technical Committee Meeting on Advances in Pellet Technology for Improved Perfromance at High Burn-up, IAEA-TEC-DEC-1036, Tokyo, October 1996, p. 245.

[13] R.F. Burstall, AEA Technology Report, ND-R-328(R), 1979.

[14] S.G. Prussin, D.R. Olander, P. Goubeault, D. Bayen, Release of volatile fission products from UO2, Proceedings of the American Nuclear Society of Topical Meeting on Fission Product Behaviour and Source Term Research, Snowbird, UT, 1984.

[15] S.G. Prussin, D.R. Olander, W.K. Lau, L. Hansson, J. Nucl. Mater. 154 (1988) 25.

[16] S.L. Hayes, J.K. Thomas, K.L. Peddicord, J. Nucl. Mater. 171 (1990) 262.

[17] S.L. Hayes, J.K. Thomas, K.L. Peddicord, J. Nucl. Mater. 171 (1990) 271.

[18] S.L. Hayes, J.K. Thomas, K.L. Peddicord, J. Nucl. Mater. 171 (1990) 289.

[19] S.L. Hayes, J.K. Thomas, K.L. Peddicord, J. Nucl. Mater. 171 (1990) 300.

[20] M.C. Billone, V.Z. Jankus, J.M. Kramer, C.I. Yang, in: J. Leary, H. Kittle (Eds.), Advanced LMFBR Fuels, Topical Meeting Proceedings, Tucson, Arizona, 1977 (ERDA).

[21] W.M. Pardue, V.W. Storhok, R.A. Smith, in: A.E. Kay, M.B. Waldron (Eds.), Plutonium 1965, Chapman and Hall, London, 1965, p. 721.

[22] H. Tagawa, J. Nucl. Mater. 51 (1974) 78.

[23] T. Matsui, R.W. Ohse, High Temp. High Press. 19 (1987) 1.

[24] Y. Arai, Y. Suzuki, T. Iwai, T. Ohmichi, J. Nucl. Mater. 195 (1992) 37.

[25] R.R. Vandervoort, W.L. Barmore, C.F. Cline, Trans. Met. Soc. AIME 242 (1968) 1466.

[26] A.A.Bauer, V.W. Storhok, Irradiation studies of (U,Pu)N, in 'Plutonium 1970 and Other Actinides', Proceedings of the Fourth International Conference on Plutonium and other Actinides, New Mexico, 5–9 October 1970, p. 532.

[27] T.B. Massalski, Binary Alloy Phase Diagrams, second Ed., vol. 1–3, ASM International, 1990.

[28] H. Holleck, Ternary phase equilibria in the systems actinide-transition metal–carbon and actinide-transition metal–nitrogen, IAEA Symposium on Thermodynamics of Nuclear Materials, Vienna 1975, p. 213.

[29] L.E. Toth, Transition Metal Carbides and Nitrides, Academic Press, New York, 1971.

[30] H. Holleck, KfK Report KfK 3087 B, January 1981.

[31] D.F. Caroll, USAEC Report HW-81603, 1965.

[32] Y.S. Touloukian (Ed.), Thermophysical Properties of High Temperature Solid Materials, vol. 5, Thermophysical Properties Research Center, Purdue University.

[33] G.V. Samsonov, I.M. Vinitskii, Handbook of Refractory Compounds, IFI/Plenum Data Company, New York, 1980.

[34] P.T.B. Shaffer, Handbooks of High Temperature Materials, No. 1 Materials Index, Plenum, New York, 1964.

[35] I. Ansara, B. Sundman, SGTE Database, in: P.S. Glaeser (Ed.), Computer Handling and Dissemination of Data, CODATA, 1987.

[36] Y. Arai, Y. Suzuki, T. Iwai, T. Ohmichi, J. Nucl. Mater. 195 (1992) 37.

[37] H. Kleykamp, J. Nucl. Mater. 275 (1999) 1.

[38] A. Languille, Private communication to M.A. Mignanelli dated 7th June 1996.

[39] H. Blank, in: R.W. Cahn et al. (Eds.), Materials Science and Technology, vol. 10A, Weinheim, New York, 1994, p. 191.

[40] Hj. Matzke, J. Chem. Soc. Faraday Trans. 86 (1990) 1243.

[41] J.S. Punni and M.A. Mignanelli, Unpublished work, 2001.

[42] J.L. Krankota and C.N. Craig, General Electric Report GEAP 13515, 1969.

[43] D.G. Martin, unpublished work, 1996.

[44] D.G. Martin, unpublished work, 1997.

[45] M.A.Mignanelli, unpublished work, 1997.

[46] Y. Arai, T. Iwai, K. Nakajima, Y. Suzuki, Recent progress of nitride fuel development in JAERI – Fuel property, irradiation behaviour and application to dry reprocessing, Proceedings of the International Conference, Global'97, Yokohama, Japan, 5–10 October 1997, vol. 1, p. 664.

[47] K. Nakajima, Y. Arai, Y. Suzuki, J. Nucl. Mater. 247 (1997) 33.

[48] N. Cocuaud, R.J.M. Konings, A. Conti, E. Picard, Hj. Matzke, Inert matrices, U-free Pu fuels and Am

targets – Synthesis of CAPRA, SPIN and EFTTRA studies, CEA Note Technique LPCA No. 61, March 1998.

[49] J.P. Charvillat, U. Benedict, D. Damien, C.H. de Novion, A. Wojakowski, W. Müller, in: W. Müller, R. Lindner (Eds.), Transplutonium elements, North Holland, Amsterdam, 1976.

[50] K. Minato, Y. Arai, M. Akabori, K. Nakajima, Research on Nitride Fuel for Transmutation of Minor Actinides, ANS Topical Meeting, AccApp/ADTTA'01, 11–15 November 2001, Reno, USA.

[51] Y. Arai, K. Nakajima, Y. Suzuki, J. Alloys Comp. 271–273 (1998) 602.